

Brownian aggregation rate of colloid particles with several active sites

Vyacheslav M. Nekrasov, Alexey A. Polshchitsin, Maxim A. Yurkin, Galina E. Yakovleva, Valeri P. Maltsev, and Andrei V. Chernyshev

Citation: *The Journal of Chemical Physics* **141**, 064309 (2014); doi: 10.1063/1.4892163

View online: <http://dx.doi.org/10.1063/1.4892163>

View Table of Contents: <http://scitation.aip.org/content/aip/journal/jcp/141/6?ver=pdfcov>

Published by the [AIP Publishing](#)

Articles you may be interested in

[Ion-specific colloidal aggregation: Population balance equations and potential of mean force](#)
J. Chem. Phys. **135**, 134704 (2011); 10.1063/1.3644769

[Transport-limited aggregation](#)
Chaos **14**, S6 (2004); 10.1063/1.1821713

[Colloidal aggregation induced by attractive interactions](#)
J. Chem. Phys. **115**, 5662 (2001); 10.1063/1.1395558

[Fractal behavior in 2-D colloidal aggregation: Structure and dynamic scaling](#)
AIP Conf. Proc. **574**, 276 (2001); 10.1063/1.1386870

[Grand canonical Brownian dynamics simulation of colloidal adsorption](#)
J. Chem. Phys. **107**, 9157 (1997); 10.1063/1.475207



AIP | Journal of
Applied Physics

Journal of Applied Physics is pleased to
announce **André Anders** as its new Editor-in-Chief

Brownian aggregation rate of colloid particles with several active sites

Vyacheslav M. Nekrasov,^{1,2} Alexey A. Polshchitsin,^{1,3} Maxim A. Yurkin,^{1,2}
 Galina E. Yakovleva,³ Valeri P. Maltsev,^{1,2,4} and Andrei V. Chernyshev^{1,2,a)}

¹Institute of Chemical Kinetics and Combustion, Institutskaya 3, 630090 Novosibirsk, Russia

²Physics Department, Novosibirsk State University, Pirogova 2, 630090 Novosibirsk, Russia

³JSC "VECTOR-BEST", PO BOX 492, Novosibirsk 630117 Russia

⁴Department of Preventive Medicine, Novosibirsk State Medical University, Krasny Prospect 52, 630091 Novosibirsk, Russia

(Received 20 June 2014; accepted 24 July 2014; published online 13 August 2014)

We theoretically analyze the aggregation kinetics of colloid particles with several active sites. Such particles (so-called "patchy particles") are well known as chemically anisotropic reactants, but the corresponding rate constant of their aggregation has not yet been established in a convenient analytical form. Using kinematic approximation for the diffusion problem, we derived an analytical formula for the diffusion-controlled reaction rate constant between two colloid particles (or clusters) with several small active sites under the following assumptions: the relative translational motion is Brownian diffusion, and the isotropic stochastic reorientation of each particle is Markovian and arbitrarily correlated. This formula was shown to produce accurate results in comparison with more sophisticated approaches. Also, to account for the case of a low number of active sites per particle we used Monte Carlo stochastic algorithm based on Gillespie method. Simulations showed that such discrete model is required when this number is less than 10. Finally, we applied the developed approach to the simulation of immunoagglutination, assuming that the formed clusters have fractal structure. © 2014 AIP Publishing LLC. [<http://dx.doi.org/10.1063/1.4892163>]

I. INTRODUCTION

Aggregation of colloids has been the subject of extensive theoretical and experimental studies due to its direct relevance to several natural processes and technological applications. Recently, colloidal particles with several active sites, so-called "patchy particles," attracted a considerable amount of interest in many applications, allowing fine tuning the directionality of the interactions for material design.¹ However, the kinetics of patchy colloids (or "functionalized colloids") aggregation and self-organization are still largely unexplored. Unfortunately, in the general case of arbitrary number of active sites with arbitrary geometry, modern sophisticated theoretical expressions for the aggregation rate of patchy particles are extremely lengthy and cumbersome (due to chemical anisotropy of the reactants), that is not convenient for treating the experimental data. The aim of the present work is therefore to derive an analytical solution, which give a simple way of calculating the rate of such sterically specific reaction with high accuracy in the most general case.

Generally, the aggregation kinetics is described theoretically by the time evolution of the clusters size distribution $C_n(t)$ (concentration of clusters of n monomers) using Smoluchowski rate equations²

$$\frac{dC_n}{dt} = \frac{1}{2} \sum_{i+j=n} k_{ij} C_i C_j - C_n \sum_{i=1}^{\infty} k_{in} C_i. \quad (1)$$

^{a)} Author to whom correspondence should be addressed. Electronic mail: chern@ns.kinetics.nsc.ru. Tel.: +7 383 3333240. Fax: +7 383 3307350.

The kernel k_{ij} represents the rate constant of the binding of i -mer with j -mer. Experimentally, the aggregation in colloids can be studied by an optical method to measure the clusters size distribution³ and to evaluate the aggregation rate constant.⁴

Two distinct classes of aggregation regimes have been investigated. One class is diffusion limited aggregation (DLA),⁵ which corresponds to a reaction occurring at each encounter between clusters. The well-known formula for the rate constant k_D of a pure diffusion-controlled binding of two chemically isotropic spherical particles is

$$k_D = 4\pi R D, \quad (2)$$

where $R = R_1 + R_2$ is the sum of the reactants radii and $D = D_1 + D_2$ is the sum of the reactants diffusion coefficients. The other class is reaction limited aggregation (RLA),⁶ where the reaction rate k_r is determined by the probability of forming a bond upon collision of two clusters. In a general case the rate constant k is often⁷ expressed by the following approximation:

$$k = \left(\frac{1}{k_D} + \frac{1}{k_r} \right)^{-1}. \quad (3)$$

Biospecific aggregation, such as immunoagglutination,⁸ is a particular case of aggregation. Biologic macromolecules are capable of sterically specific (chemically anisotropic) binding with particular ligands.⁹ The reactants can bind to each other only at certain discrete reactive spots (active sites), which are relatively small comparing to the size of reactants. Therefore, one can expect significant steric factor for aggregation kinetics, since specific binding sites occupy a rather

small surface fraction of a particle. It is generally believed that the activation energy for the association reaction between ligand and receptor is rather low. Therefore, the reaction rate of biospecific aggregation can be calculated in the diffusion limited regime taking into account a steric factor, which reduces the DLA rate constant. For example, the DLA rate constant of binding of chemically isotropic ligands with a chemically anisotropic spherical particle covered by receptors can be approximately expressed by the following formula:¹⁰

$$k = \left[\frac{1}{k_D} + \frac{1-p}{4DaN} \right]^{-1}, \quad (4)$$

where p is the fraction of the particles surface covered by receptors binding sites, a is the size (radius) of the binding site, N is the number of binding sites on the particle. Equation (4) is formally similar to Eq. (3) that often leads to interpretation of sterically specific DLA as “pseudo-RLA.” Pseudo-RLA can be distinguished experimentally from pure RLA due to its strong dependence on the viscosity of the media (through the diffusion coefficient). Discrimination of sterically specific DLA from pure RLA is very important for the determination of the binding site characteristics (size, shape, etc.) and the number of binding sites (receptors) on the particle from experimental data, as well as for the theoretical simulation of the aggregation kinetics.

It should be noted that the reaction-diffusion problem of chemically anisotropic reactants in condensed phase received considerable theoretical attention.¹⁰⁻¹⁷ In a general case it is convenient to introduce an effective factor $F \leq 1$ which describes the reduction of the reaction rate compared to the pure DLA:

$$k = 4\pi R D F. \quad (5)$$

The problem can be formulated as follows: given the structural characteristics of the reactants, determine the effective factor F for diffusing and rotating molecules. Here we will always consider rotational diffusion as a Markovian stochastic reorientation process of sufficiently large particle in dense media.¹⁴ For simplicity, both reactants are considered spherical (Fig. 1). The rate of diffusion-controlled reaction on binding sites exhibit quite unexpected behavior, caused by the cage effect (every encounter of two reactants consists of numerous recontact collisions). For example, if the first reactant

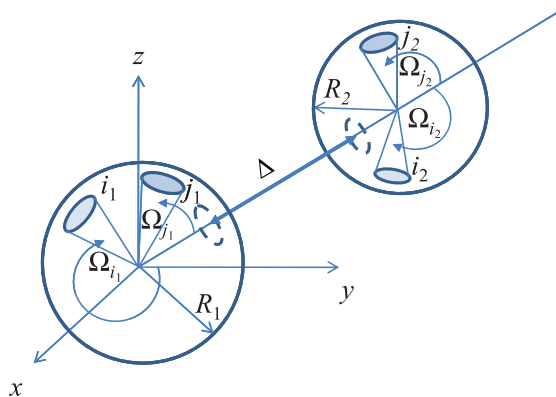


FIG. 1. Spatial configuration of two chemically anisotropic reagents.

is a spherical particle with one small circular reactive spot on its surface with steric factor (surface fraction) $f \ll 1$ and the second reactant is a spherical particle with isotropic reactivity, the forward rate constant of the binding is, counterintuitively, proportional to \sqrt{f} but not to f .^{7,13} Only at $f \sim 1$ the binding rate constant becomes proportional to f . However, the generalization of this result to chemically anisotropic reactants, based on the equation for diffusion in multidimensional space (including angular variables of both particles) with corresponding boundary conditions, remains a severe mathematical problem even for numerical methods.^{18,19} This fact has stimulated an active search for physical approximations that could further simplify the problem.^{13,20} The most promising approach is based on the “kinematic approximation,”^{13,14,17,21} which allows the rate constant to be calculated from the motion parameters in the configuration space of the nonreactive partners under the assumption that the thickness of reaction zone (i.e., maximum distance between the particles when the reaction occurs) is $\Delta \ll R$.

If each reactant has a reactive spot (with the steric factor f_i from 0 to 1), the applicability of the kinematic approximation has been mathematically substantiated,¹³ giving the expression

$$k = V/\tau, \quad (6)$$

where V is the reactive zone volume:¹⁴

$$V = 4\pi R^2 f_1 f_2 \Delta. \quad (7)$$

Here f_1 and f_2 are steric factors of the first and second reactants, correspondingly, and τ is the total residence time of the system representation point inside the reactive zone:¹⁴

$$\tau = \int_{q \in V} \int_{q_0 \in V} G(q; q_0) dq_0 dq / \int_{q_0 \in V} dq_0, \quad (8)$$

where $G(q; q_0)$ is the Green function of stochastic motion of the reactants. In Eq. (8) integration is performed over the complete set of configurational variables q , and averaging goes over their initial values q_0 within the reaction zone (Fig. 1). Unfortunately, in the case of two anisotropic reactants, the Green function $G(q; q_0)$ is fairly cumbersome¹⁴ and demands certain numerical efforts that force researchers to use more simple approximations (e.g., the so-called quasi-chemical approximation^{12,19,22}) to compute the rate constant with significantly lower accuracy. Therefore, a proper analytical (simple) expression which approximates the rate constant obtained numerically with Eqs. (6)–(8) for a particular application without essential loss of accuracy is still required in order to make the kinematic approximation more applicable in practice. In this paper we derive such an expression for the case of two spherical anisotropic reactants.

Another important question concerns the reactive spot shape available for the approximation represented by Eqs. (6)–(8) in the framework of the kinematic approximation.¹⁷ The precision of the kinematic approximation was shown¹³ to be good for the case of one small circular reactive spot on the first spherical reactant and the isotropic reactivity of the second reactant, since the inverse diffusion problem can be analytically solved only in this case.

Then the applicability of the kinematic approximation was extended to the reactive spot of arbitrary shape.^{14,17} However, recent publication¹⁵ on “multi-spot” reactants raised the question on the limits of the spot shapes suitable for the kinematic approximation. In that publication¹⁵ the authors considered the case of several reactive spots on the first reactant and the isotropic reactivity of the second reactant. Obviously, this case can be considered as a single reactive spot of arbitrary shape, specifically the “multi-spot shape.” But the authors considered this case differently applying the following expression for the rate constant instead of Eq. (6):

$$k = \sum_i \sum_j K_{ij}, \quad (9)$$

where matrix \mathbf{K} is the inverse matrix of \mathbf{G} :

$$\mathbf{K} = \mathbf{G}^{-1}, \quad (10)$$

$$G_{ij} = \frac{1}{\Omega_i \Omega_j} \int_{\Omega_i} \sin \theta_i d\theta_i d\varphi_i \int_{\Omega_j} G(\theta_i, \varphi_i; \theta_j, \varphi_j) \sin \theta_j d\theta_j d\varphi_j, \quad (11)$$

where i and j are the indexes of the reactive spots on the anisotropic reactant, θ_i and φ_i are the spherical angular variables within the solid angle Ω_i of the spot i (see Fig. 1). Obviously, the results of Eqs. (6) and (9) are generally different. One can argue that the difference is due to the assumption of the connected spot, inherent in Eq. (6). However, there is a simple counter-evidence: it is possible to add infinitely narrow connected strips (of reactive area) between the spots to make the whole shape connected with no effect on the rate constant. Thus, the open question appeared is the following: how much is the difference between the results of the Eqs. (6) and (9) for the “multi-spot” shape? In this paper we numerically compare these two methods and show that the difference is not much and is negligible for many applications. Also, we compare the results of Eqs. (6) and (9) with literature data on numerical stochastic motion simulations²³ and also with known analytical formulas^{10,16} for the case of “isotropic”– “multispot anisotropic” pair. Unfortunately, to the best of our knowledge there is no similar analytical approximate formula in the general case of anisotropic-anisotropic pair for the rate constant depending on the number and size of reactive spots on both reactants of different radii. Such formula would be very useful to simulate the kinetics of biospecific receptor-mediated aggregation with Eq. (1). Simple analytical expressions for rate kernels of Smoluchowski equation should increase the speed of computation of the clusters population dynamics. Moreover, rapid computation of such direct kinetic problem is very important to be able to solve the inverse problem (e.g., to find the size of the reactive spots from the experimentally observed dynamics of the colloid population) in reasonable time.

In this paper we suggest an approximate analytical formula for the diffusion controlled rate constant in the case of the “multispot-multispot” pair of reactants. We always assume that all spots have the same size, and the spot size is much less than the distance between spots. Applying Monte Carlo approach, we also show the specific behavior of the aggregation kinetics curve, caused by discreteness of receptors, i.e., due to a finite number of them on a single particle.

II. ISOTROPIC-ANISOTROPIC PAIR

Let us first consider the case when the first reactant of radius R_1 is chemically isotropic and the second reactant of radius R_2 is chemically anisotropic with N small identical reactive circular spots of the radius $a \ll R$ and the steric factor $f \ll 1$ on its surface. Here and further the steric factor is defined for a single spot. A few analytical approximate formulae for the diffusion controlled rate constant^{10,16} supported by Brownian dynamics numerical simulation method of Northrup²³ are known in the literature for this case:

(1) Berg and Purcell equation:¹⁶

$$k = \left[\frac{1}{4\pi R D} + \frac{1}{4DaN} \right]^{-1}. \quad (12)$$

(2) Zwanzig equation:¹⁰

$$k = \left[\frac{1}{4\pi R D} + \frac{1 - Na^2/(4R^2)}{4DaN} \right]^{-1}. \quad (13)$$

We applied two variants of the kinematic approximation to calculate the rate constant neglecting rotational diffusion: (1) single-spot approach¹³ by Eq. (6) and (2) multi-spot approach¹⁵ by Eq. (9), using the following Green function¹³ of the external Neumann problem for a sphere with radius R with implicit assumption $\Delta \ll R$:

$$G(\theta_i, \varphi_i; \theta_j, \varphi_j) = \frac{1}{4\pi R D} \left\{ \frac{\sqrt{2}}{\sqrt{1 - \cos \gamma}} - \ln \left[1 + \frac{\sqrt{2}}{\sqrt{1 - \cos \gamma}} \right] \right\}, \quad (14)$$

$$\cos \gamma = \cos \theta_i \cos \theta_j + \sin \theta_i \sin \theta_j \cos(\varphi_i - \varphi_j). \quad (15)$$

We found (see an example in Fig. 2 for $f^{1/2} = a/2R = 0.0314$) that both variants of the “kinematic approximation” give similar results, which are close to the known analytical formulas for the rate constant in the isotropic-anisotropic case. This result supports the traditional assumption of the arbitrary (even “multi-spot”) shape of the reactive zone available for the rate constant calculations by the “kinematic approximation.”

Let us, however, investigate this issue in more details. For a single spot the factor F can be presented for this case as follows:¹⁴

$$F = [1 + F_2^{-1}]^{-1}, \quad (16)$$

where F_2 is the factor, accounting for the chemical anisotropy of the second reactant, i.e., it corresponds to the very small reactive zone. By contrast, term “1” corresponds to large spot, up to the whole spherical surface. For a small circular spot F_2 is equal to¹⁴

$$F_2^{(1)} = \frac{3\pi}{16} f^{1/2}, \quad (17)$$

where superscript (1) in $F_2^{(1)}$ denotes single-spot case.

Let us now consider the reactive zone as an ensemble of circular spots of equal sizes, much smaller than the distance

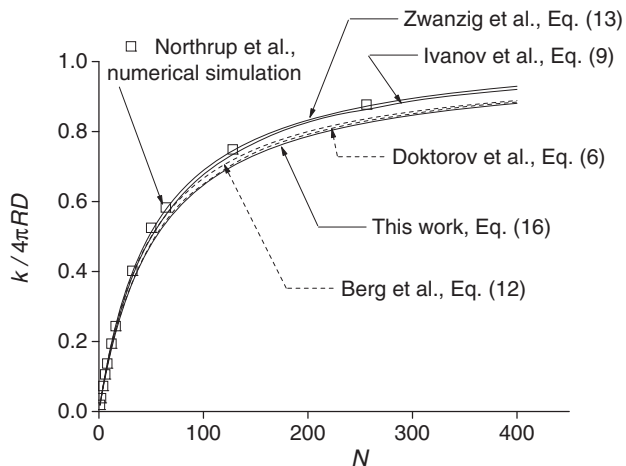


FIG. 2. The rate constant calculation by different methods for the isotropic-anisotropic case at $f^{1/2} = a/2R = 0.0314$.

between spots. Then one can split the integral over the Green function in Eq. (8) into self- and cross-terms leading to the following expression for the rate constant (according to Eq. (6)):

$$\begin{aligned} \frac{1}{k} &= \frac{1}{V^2} \int \int_{q \in V, q_0 \in V} G(q; q_0) dq_0 dq \\ &= \frac{1}{V^2} \sum_{\substack{i,j=1 \\ i \neq j}}^N G_{ij} + \frac{1}{V^2} \sum_{i=1}^N G_{ii}, \end{aligned} \quad (18)$$

where $V = NV_i = N\Omega_i R^2 \Delta$. Since the small reactive spots are randomly spatially distributed on the spherical surface, one can estimate the average (over all possible spatial locations of the spots on the surface) value of the first term of Eq. (18) through the integral of the Green function over the whole spherical surface (taking into account the definition of the Green function):

$$\begin{aligned} \left\langle \frac{1}{V^2} \sum_{\substack{i,j=1 \\ i \neq j}}^N G_{ij} \right\rangle &= \frac{N(N-1)V_i^2}{V^2} \frac{1}{4\pi R} \oint G(q; q_0) dq \\ &= \frac{(N-1)}{N} \frac{1}{4\pi RD} \approx \frac{1}{4\pi RD}. \end{aligned} \quad (19)$$

The second term of Eq. (18) can be represented through F_2 factor as follows:

$$\frac{1}{V^2} \sum_{i=1}^N G_{ii} = \frac{1}{4\pi RD} F_2^{-1} \quad (20)$$

that leads to expression (16) mentioned above for the steric factor F . One can see that the sum over cross-terms and self-terms in Eq. (18) corresponds to 1 and F_2 in Eq. (16), respectively. If only self-terms are considered, the problem scales down to that of a single spot:

$$F_2 = NF_2^{(1)} = \frac{3\pi}{16} Nf^{1/2}. \quad (21)$$

This correspondence is rigorous when $Nf^{1/2} \ll 1$ – then the sum over cross-terms can be neglected and $F_2 \approx F$ because

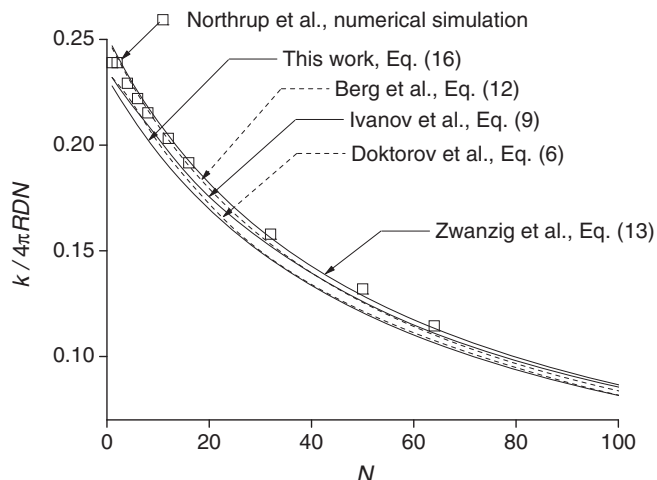


FIG. 3. Same as Fig. 2 but for $N < 100$ and with additional normalization of k by N .

they are both much smaller than 1. The system is then in the pseudo-RLA limit and reactive spots are independent. Thus, the total rate constant is the sum of N partial rate constants on individual spots. One can see in Fig. 2, that combination of Eqs. (16) and (21) provides a good approximation of the total rate constant in the wide range from the extreme case of strong anisotropy to the case of a pure isotropy of the second reactant. Moreover, it better agrees with Ivanov *et al.*¹⁵ for small N than other analytical approximations (Fig. 3). The remaining difference (even for $N = 1$) is due to the approximate Eq. (17) in contrast to the exact evaluation of Green-tensor integral by both Eqs. (6) and (9).

Another implication of assumption $Nf^{1/2} \ll 1$ is that matrix \mathbf{G} and, hence, matrix \mathbf{K} are diagonally dominant; cf. Eq. (18). This, in turn, implies equivalence of Eqs. (6) and (9) in this regime, which is also supported by Fig. 2.

Finally, Eq. (21) can be further modified by accounting for the rotational diffusion (both the rotational and translational frictions are of the Stokes type). This is implemented by an additional multiplicative factor¹⁴

$$F_2 = \frac{3\pi}{16} Nf^{1/2} \left(1 + \frac{3R_1}{4R_2} \left(1 + \frac{R_1}{R_2} \right) \right)^{1/2}, \quad (22)$$

where R_1 and R_2 are radii of isotropic and anisotropic reactants, respectively.

III. ANISOTROPIC-ANISOTROPIC PAIR

In this case the first reactant of radius R_1 has N_1 small reactive circular spots of equal steric factor $f_1 \ll 1$ and the second reactant of radius R_2 has N_2 small reactive circular spots of equal steric factor $f_2 \ll 1$. To the best of our knowledge, the case of the anisotropic-anisotropic pair of multi-spot reactive zones on both reactants has not been discussed in the literature from the point of view of a simple analytical approximate formula for the rate constant depending on the number and the

size of reactive spots on both particles of different radii. In order to derive such a formula we will use the presentation of the effective factor F in the form¹⁴

$$F = [1 + F_1^{-1} + F_2^{-1} + F_{12}^{-1}]^{-1}, \quad (23)$$

derived for a single reactive spot on each reactant. Similar to Eq. (16) the factors F_1 , F_2 , and F_{12} correspond to the following extreme cases (depending on the degree of the anisotropy of the reactants): F_1 – first reactant is extremely anisotropic and second reactant is isotropic; F_2 – first reactant is isotropic and second reactant is extremely anisotropic; F_{12} – both reactants are extremely anisotropic. The factors $F_1^{(1)}$ and $F_2^{(1)}$ (superscripts denote single-spot case) correspond to the case of Sec. II and, therefore, can be obtained from Eq. (22) with proper change of indices. The factor $F_{12}^{(1)}$ (superscript (1) denotes the case of a single spot on each reactant) can be computed using the known but cumbersome expression¹⁴ of the kinematic approximation

$$F_{12}^{(1)} = (f_1\sqrt{f_2} + f_2\sqrt{f_1}) h(\sqrt{f_1/f_2}), \quad (24)$$

$$[h(\xi)]^{-1} = (1 + \xi) \int_0^\infty \int_0^\infty \frac{dx dy}{xy} \frac{J_1^2(x) J_1^2(y)}{w^{1/2}(x, y, \xi)} K \left[\frac{4\xi xy}{w(x, y, \xi)} \right], \quad (25)$$

$$w(x, y, \xi) = (x + \xi y)^2 + 4f_2\xi^2 S^2 \left(\frac{x}{2f_1^{1/2}}; \frac{y}{2f_2^{1/2}} \right), \quad (26)$$

$$S^2(\mu, \nu) = \frac{R^2}{D} [\mu(\mu + 1)D_{rot}^{(1)} + \nu(\nu + 1)D_{rot}^{(2)}], \quad (27)$$

where K is an elliptic integral; J_1 is Bessel function of the first kind; $D_{rot}^{(1)}$ and $D_{rot}^{(2)}$ are the rotation diffusion coefficients of the first and the second reactants, correspondingly. We consider only two specific cases of rotational diffusion. First case is for no rotational diffusion, i.e., $S = 0$, which is further denoted by subscript 0. In particular, $w_0(x, y, \xi) = (x + \xi y)^2$ and $h_0(0) = 3\pi/16$; cf. Eq. (17). Second case (the default one) is for the Stokes rotational diffusion (same as translational)

$$D_{rot}^{(j)} = \frac{k_B T}{8\pi\eta R_j^3}, \quad D = \frac{k_B T}{6\pi\eta} \left(\frac{1}{R_1} + \frac{1}{R_2} \right). \quad (28)$$

Here and further we assume that the size of the reactive spot is the same on both reactants, i.e., $f_1 R_1^2 = f_2 R_2^2$, and neglect “+1” in the brackets in Eqs. (27) and (28). Then,

$$w(x, y, \xi) = (x + \xi y)^2 + \frac{3}{4}(1 + \xi)(\xi x^2 + y^2), \quad (29)$$

and $h(\xi)$ depends solely on its argument. One can easily show that $h(\xi) = h(1/\xi)$, which corresponds to the symmetry of $F_{12}^{(1)}$ with respect to interchange of the reactants. Hence, one need to know $h(\xi)$ and $h_0(\xi)$ only for $0 \leq \xi \leq 1$. We have calculated both these functions in this range using quasi Monte Carlo integration with relative errors less than 10^{-3} , results are shown in Fig. 4. Variability of these functions is within

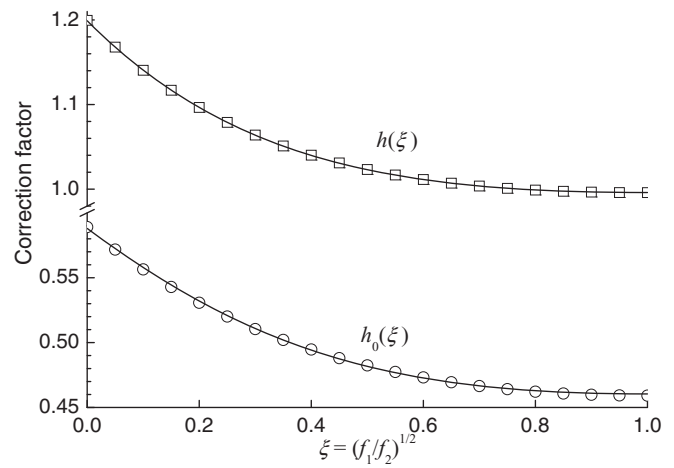


FIG. 4. The correction factors $h(\xi)$ and $h_0(\xi)$: dots – calculated by direct numerical integration; solid line – approximation (30).

25% over the whole range, so they can be considered constant in the zero approximation. Alternatively, the following interpolating formulae can be used:

$$h(\xi) = 1.199 \frac{1 + 0.708\xi + \xi^2}{1 + 1.206\xi + \xi^2}, \quad (30)$$

$$h_0(\xi) = 0.588 \frac{1 - 0.044\xi + \xi^2}{1 + 0.498\xi + \xi^2}.$$

These formulae keep the original symmetry and have relative errors less than 3×10^{-3} .

To accommodate multiple spots we consider the reactive zone on each reactant as an ensemble of circular spots of equal sizes, and the size of the spot is much smaller than the distance between spots. Then we split the integral over the Green function in Eq. (8), similar to Eq. (18):

$$\frac{1}{k} = \frac{1}{V_1^2 V_2^2} \left(\sum_{\substack{i,j=1 \\ i \neq j}}^{N_1} \sum_{\substack{\mu,\nu=1 \\ \mu \neq \nu}}^{N_2} G_{ij}^{\mu\nu} + \sum_{i=1}^{N_1} \sum_{\substack{\mu,\nu=1 \\ \mu \neq \nu}}^{N_2} G_{ii}^{\mu\nu} + \sum_{\substack{i,j=1 \\ i \neq j}}^{N_1} \sum_{\mu=1}^{N_2} G_{ij}^{\mu\mu} + \sum_{i=1}^{N_1} \sum_{\mu=1}^{N_2} G_{ii}^{\mu\mu} \right), \quad (31)$$

$$G_{ij}^{\mu\nu} = \frac{1}{\Omega_i^{(1)} \Omega_\mu^{(2)} \Omega_j^{(1)} \Omega_\nu^{(2)}} \int_{\Omega_i^{(1)}} d\omega^{(1)} \int_{\Omega_\mu^{(2)}} d\omega^{(2)} \int_{\Omega_j^{(1)}} d\omega_0^{(1)} \times \int_{\Omega_\nu^{(2)}} d\omega_0^{(2)} G(\omega^{(1)}, \omega^{(2)}; \omega_0^{(1)}, \omega_0^{(2)}), \quad (32)$$

where i, j and μ, ν index spots on reactant 1 and 2, respectively, and ω denote angular variables varying over the corresponding spot surfaces (solid angles Ω). Green function inside integral in Eq. (32) is very cumbersome,¹⁴ which makes direct analysis of $G_{ij}^{\mu\nu}$ non-trivial. Instead we resort to correspondence between cross-terms ($i \neq j$ and/or $\mu \neq \nu$) and the

result for the isotropic reactant, discussed in Sec. II. Thus,

$$\left\langle \frac{1}{V_1^2 V_2^2} \sum_{\substack{i,j=1 \\ i \neq j}}^{N_1} \sum_{\substack{\mu,\nu=1 \\ \mu \neq \nu}}^{N_2} G^{\mu\nu}_{ij} \right\rangle = \frac{(N_1 - 1)(N_2 - 1)}{N_1 N_2} \frac{1}{4\pi R D} \approx \frac{1}{4\pi R D}, \quad (33)$$

$$\left\langle \frac{1}{V_1^2 V_2^2} \sum_{i=1}^{N_1} \sum_{\substack{\mu,\nu=1 \\ \mu \neq \nu}}^{N_2} G^{\mu\nu}_{ii} \right\rangle = \frac{N_2 - 1}{N_1 N_2} \frac{1}{4\pi R D F_1^{(1)}} \approx \frac{1}{4\pi R D N_1 F_1^{(1)}}, \quad (34)$$

$$\left\langle \frac{1}{V_1^2 V_2^2} \sum_{\substack{i,j=1 \\ i \neq j}}^{N_1} \sum_{\mu=1}^{N_2} G^{\mu\mu}_{ij} \right\rangle = \frac{N_1 - 1}{N_1 N_2} \frac{1}{4\pi R D F_2^{(1)}} \approx \frac{1}{4\pi R D N_2 F_2^{(1)}}, \quad (35)$$

$$\frac{1}{V_1^2 V_2^2} \sum_{i=1}^{N_1} \sum_{\mu=1}^{N_2} G^{\mu\mu}_{ii} = \frac{1}{4\pi R D N_1 N_2 F_{12}^{(11)}}. \quad (36)$$

Finally, Eq. (31) term-by-term corresponds to Eq. (23) with

$$F_1 = N_1 F_1^{(1)} = \frac{3\pi}{16} N_1 f_1^{1/2} \left(1 + \frac{3R_2}{4R_1} \left(1 + \frac{R_2}{R_1} \right) \right)^{1/2}, \quad (37)$$

$$F_2 = N_2 F_2^{(1)} = \frac{3\pi}{16} N_2 f_2^{1/2} \left(1 + \frac{3R_1}{4R_2} \left(1 + \frac{R_1}{R_2} \right) \right)^{1/2}, \quad (38)$$

$$F_{12} = N_1 N_2 F_{12}^{(11)} = N_1 N_2 \left(f_1 \sqrt{f_2} + f_2 \sqrt{f_1} \right) h \left(\sqrt{f_1/f_2} \right). \quad (39)$$

Similar to Sec. II the combination of Eqs. (23) with (37)–(39) is expected to be adequate for the whole range of N_1 and N_2 . Moreover, the whole derivation is rigorous in the limit of $F_{12} \ll \min(F_1, F_2, 1)$, which is equivalent to

$$N_1 f_1 \ll 1, \quad N_2 f_2 \ll 1, \quad N_1 N_2 \left(f_1 \sqrt{f_2} + f_2 \sqrt{f_1} \right) \ll 1, \quad (40)$$

which is significantly weaker than the requirement for each reactant independently when the other reactant is considered isotropic. This is a consequence of accounting for rotational diffusion. Obviously, Eq. (40) implies $F \approx F_{12}$.

IV. IMMUNOAGGLUTINATION

If the receptors-covered particles in colloid are surrounded by dissolved multivalent ligand molecules, the aggregation (i.e., immunoagglutination) is going on due to the formation of receptor-ligand-receptor “bridges” between the particles. Immunoagglutination means that there are two types of receptors on the surface of the particles (1) free receptors and (2) receptors occupied by ligand, and the binding

is possible only between free and occupied receptors. Let the first particle has on its surface $N_{x,1}$ free receptors and $N_{y,1}$ occupied receptors, and, correspondingly, the second particle has $N_{x,2}$ and $N_{y,2}$ surface receptors. Although the above derivation provides a general framework, below we limit ourselves to the case of Eq. (40). Then one can use Eq. (39) for the effective steric factor F and obtain the following analytical expression for the binding rate constant:

$$k = 4\pi R D \left(f_1 \sqrt{f_2} + f_2 \sqrt{f_1} \right) \times (N_{x,1} N_{y,2} + N_{y,1} N_{x,2}) h \left(\sqrt{f_1/f_2} \right). \quad (41)$$

V. MODELING CLUSTERS AS FRACTAL OBJECTS

We assume that all monomers are spherical particles of the same radius $R^{(1)}$ and total number $N^{(1)}$ of receptors on the surface. In order to apply the above results for the simulation of the aggregation kinetics we consider the clusters as fractal particles²⁴ also of spherical shape. That means the radius $R^{(i)}$ of a cluster consisting of i monomers can be expressed through the monomer radius, as follows:

$$R^{(i)} = R^{(1)} i^{1/d}, \quad (42)$$

where d is the fractal dimension (in the range from 2 to 3) of the cluster. We assume that the average surface density of all receptors on clusters is not changing during aggregation and the cluster surface available to binding is equal to that of the equivalent sphere. Then the total number $N^{(i)}$ of surface receptors on a cluster of size i is

$$N^{(i)} = N^{(1)} i^{2/d}. \quad (43)$$

Due to steric complementarity (i.e., biospecificity) of the ligand and the receptor, their corresponding reactive spots are equal in size (e.g., the effective radius of the spot). Let a be the effective radius of the reactive spot. Then the steric factor $f^{(i)}$ of the reactive spot of the cluster is

$$f^{(i)} = \left(\frac{a}{2R^{(1)}} \right)^2 i^{-2/d}. \quad (44)$$

Diffusion coefficient $D^{(i)}$ of the cluster can be approximated using the Stokes-Einstein formula

$$D^{(i)} = \frac{k_B T}{6\pi \eta R^{(i)}} = \frac{k_B T i^{-1/d}}{6\pi \eta R^{(1)}}, \quad (45)$$

where η is the viscosity of the media, k_B is the Boltzmann constant, T is the temperature.

If one neglects stochastic variation of the fraction p of occupied surface receptors from particle to particle (due to a finite number of receptors), then each particle (monomer or cluster) has certain number of free $N_{x,n}^{(i)}$ and occupied $N_{y,n}^{(i)}$ receptors on their surface:

$$N_{x,n}^{(i)} = N_x^{(1)} i^{2/d} = (1 - p) N^{(1)} i^{2/d}, \quad (46)$$

$$N_{y,n}^{(i)} = N_y^{(1)} i^{2/d} = p N^{(1)} i^{2/d}. \quad (47)$$

Let us denote this model as continuous one. Substituting Eqs. (46) and (47) into Eq. (41) and taking into account

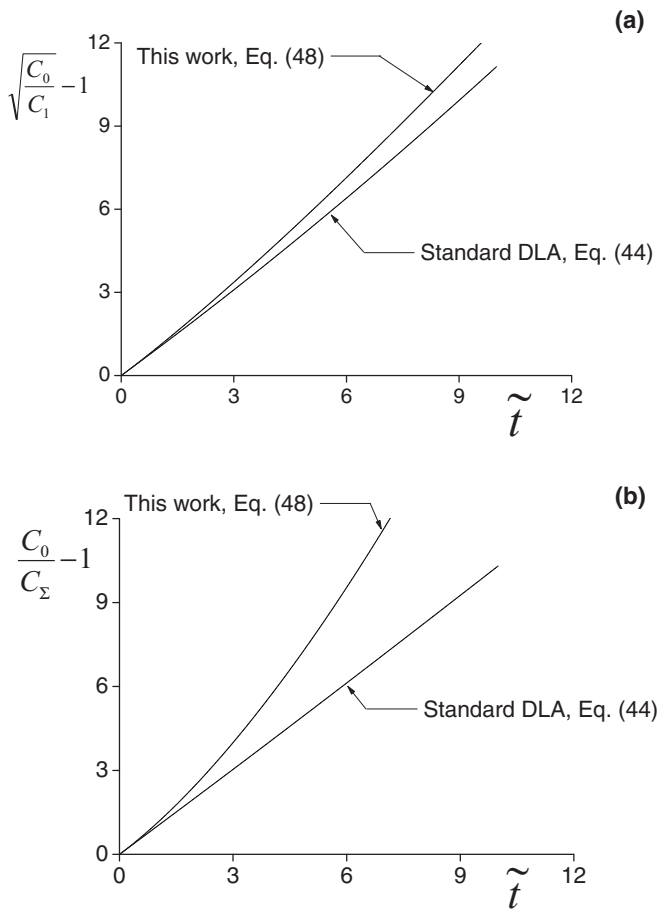


FIG. 5. Theoretical kinetics neglecting discreteness of receptors on particles for standard DLA and for our rate kernels of Smoluchowski equation (continuous model, Eq. (48)).

Eqs. (42)–(45), the binding rate constant k_{ij} between two clusters can be expressed as

$$k_{ij} = \frac{4k_B T}{3\eta} \left(\frac{a}{2R^{(1)}} \right)^3 N_x^{(1)} N_y^{(1)} (i^{1/d} + j^{1/d})^2 \times (i^{-1/d} + j^{-1/d}) h((i/j)^{1/d}). \quad (48)$$

Assuming that at start time ($t = 0$) of aggregation there were only monomers with the initial concentration C_0 , we simulated the aggregation kinetics by Smoluchowski Eq. (1) using two different kernels: (1) k_{ij} from Eq. (48); and (2) standard DLA kernel²⁵

$$k_{ij}^{DLA} = \frac{2k_B T}{3\eta} (i^{1/d} + j^{1/d})(i^{-1/d} + j^{-1/d}), \quad (49)$$

assuming $d = 3$. The results of the simulation are shown in Fig. 5 in terms of the relative time

$$\tilde{t} = \frac{1}{2} k_{11} C_0 t. \quad (50)$$

For the illustration we present the kinetics of monomers C_1 (Fig. 5(a)) and all particles C_Σ (Fig. 5(b)) using traditional coordinate transforms: $y = \sqrt{C_0/C_1} - 1$,²⁶ and $y = C_0/C_\Sigma - 1$,²⁷ since they are linear in time for the particular case of a constant kernel ($k_{ij} = \text{const}$) of Smoluchowski Eq. (1) and almost linear for the standard DLA. Use of relative

time allows us to separate the effect of different dependence on i and j (in contrast to different prefactors). In particular, our model predicts faster binding of larger clusters relative to the smaller ones (e.g., for $i = j$), which results in cumulative increase of aggregation speed.

VI. MONTE CARLO SIMULATION OF BIOSPECIFIC AGGREGATION

In this section we build up a “discrete” aggregation model (in contrast to the continuous model used in Sec. V), taking into account the finite number of receptors on each particle. This implies stochastic variation of the fraction of occupied receptors from particle to particle described by the binomial distribution

$$P(N_y; N, p) = \frac{N!}{(N_y)!(N - N_y)!} p^{N_y} (1 - p)^{N - N_y}, \quad (51)$$

where $P(N_y; N, p)$ is the probability for the particle with N total surface receptors to have N_y occupied surface receptors if the average fraction of occupied surface receptors is p . This variation is especially important for $Np \sim 1$.

We used the following algorithm for the population dynamics simulation. At the beginning of the process all particles are monomers which are stochastically distributed on the

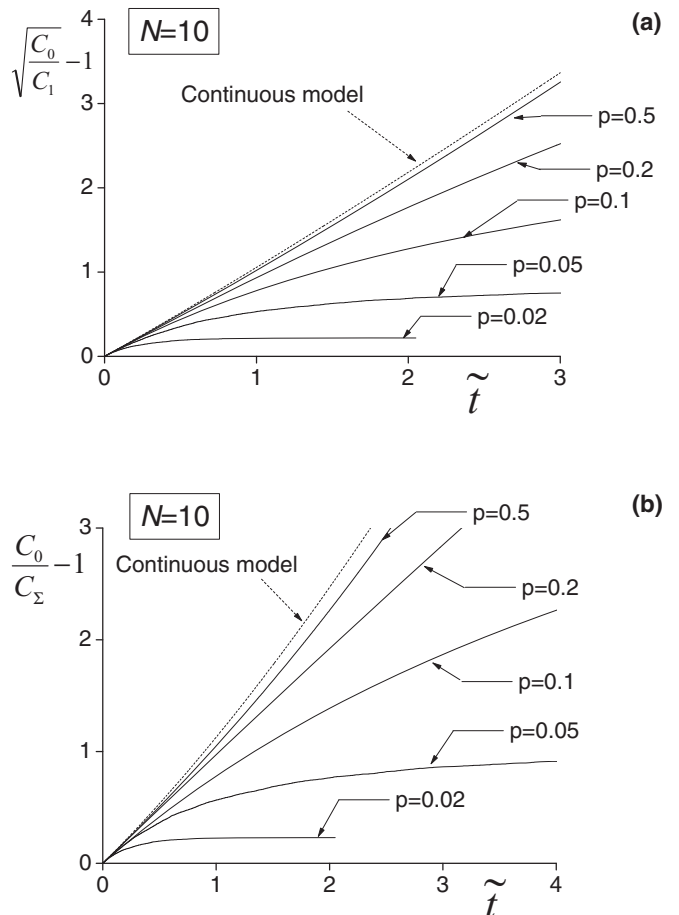
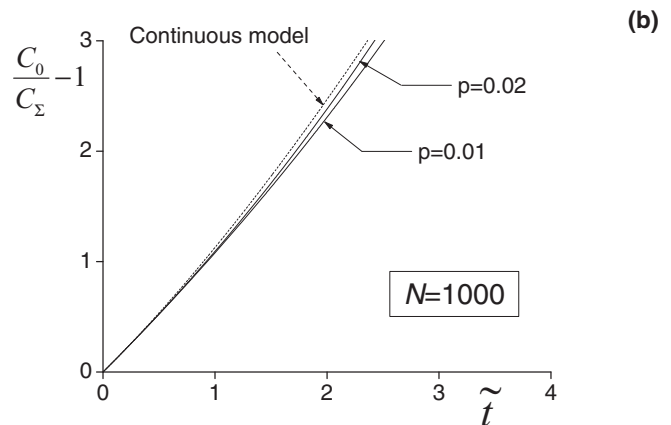
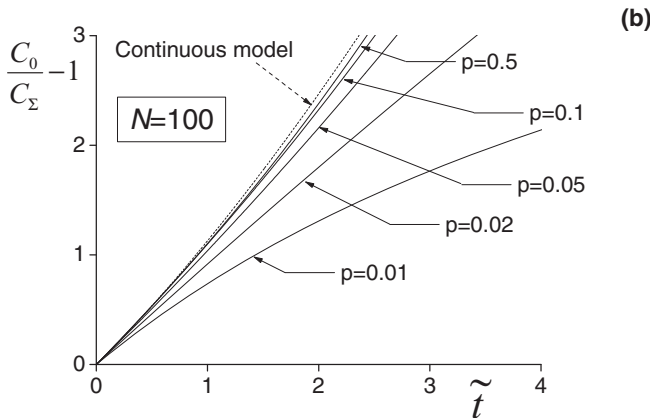
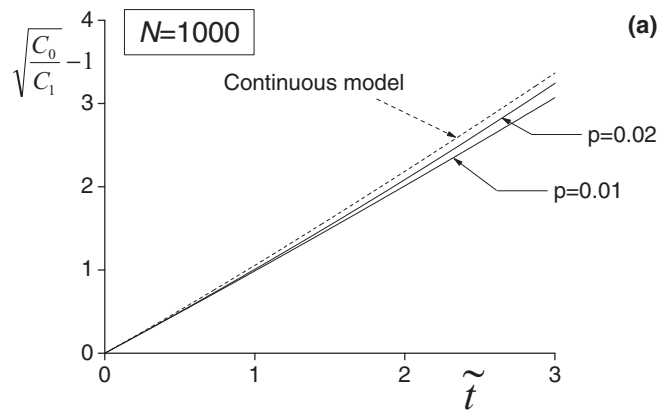
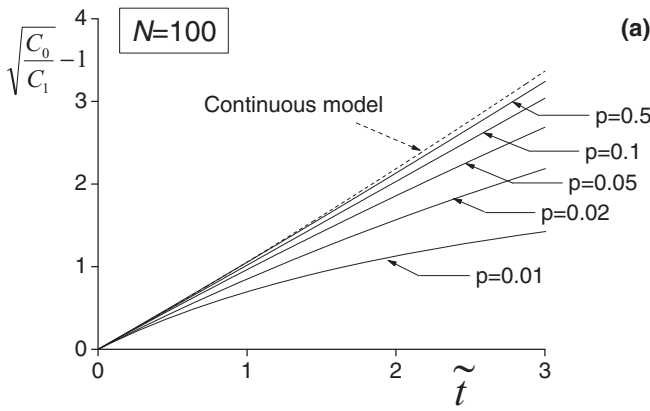


FIG. 6. Theoretical kinetics taking into account discreteness of receptors on particles (at $N = 10$ and different p), and the comparison with the continuous model (Eq. (48)).

FIG. 7. Same as Fig. 6 but for $N = 100$.FIG. 8. Same as Fig. 6 but for $N = 1000$.

amount of occupied receptors according to Eq. (51). In order to apply Eq. (41) for the simulation one has to know the numbers of free $N_{x,n}^{(i)}$ and occupied $N_{y,n}^{(i)}$ receptors on the reactants ($n = 1, 2$) surface. Due to the fractal structure of the clusters,

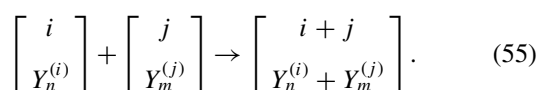
$$N_{x,n}^{(i)} = 4\pi R^{(i)^2} \frac{X_n^{(i)}}{4\pi R^{(1)^2} i} = X_n^{(i)} i^{(2/d)-1}, \quad (52)$$

$$N_{y,n}^{(i)} = 4\pi R^{(i)^2} \frac{Y_n^{(i)} - (i-1)}{4\pi R^{(1)^2} i} = [Y_n^{(i)} - (i-1)] i^{(2/d)-1}, \quad (53)$$

where $Y_n^{(i)}$ and $X_n^{(i)}$ are the total number of ligand molecules and free receptors in the cluster (both on the surface and inside) consisting of i monomers. The term $(i-1)$ in Eq. (53) is the number of bonds between i monomers in the cluster. Taking into account that all monomers have the same total number $N^{(1)}$ of surface receptors one can calculate $X_n^{(i)}$ through $Y_n^{(i)}$:

$$X_n^{(i)} = iN^{(1)} - Y_n^{(i)} - (i-1). \quad (54)$$

Let us denote the particle number n (monomer or cluster) by the vector $[Y_n^{(i)}]$. Then the reaction scheme can be expressed as



The rate constant of reaction (55) is calculated substituting Eqs. (52)–(54) into Eq. (41).

Thus, the population of particles in the colloid system is represented by the particles concentration $C(i, Y_n^{(i)}; t)$ as a function of i and $Y_n^{(i)}$ at certain time t . During the aggregation the function $C(i, Y_n^{(i)}; t)$ is changing according to the reaction scheme (55). Using initial condition based on Eq. (51)

$$C(i, Y_n^{(i)}; t=0) = \begin{cases} C_0 P(Y_n^{(1)}; N^{(1)}, p), & i=1, \\ 0, & i>1, \end{cases} \quad (56)$$

we calculated the population dynamics $C(i, Y_n^{(i)}; t)$ using Monte Carlo stochastic simulation algorithm (SSA) of Gillespie^{28,29} modified for aggregation.³⁰ Since the aggregating system is strongly coupled, we chose the direct SSA method.^{29,31}

Theoretical kinetics of the aggregation, which we simulated taking into account discrete number of receptors on particles, are shown in Figs. 6–8. One can see from these figures that the discreteness on the reactive spots affects significantly the aggregation kinetics, if the number of reaction zones (free binding sites) on a monomer particle is less than 10 (i.e., the product $pN < 10$ or $(1-p)N < 10$).

VII. CONCLUSION

Using kinematic approximation of the diffusion problem we derived a new analytical formula for the rate constant of

aggregation in the general case when both reactants of different radii have arbitrary number of reactive spots (active sites). The formula was extended to the case when receptors are partially occupied by multivalent ligands (immunoagglutination). The clusters were modeled as fractal objects of spherical shape. Applying this formula for the simulation of the biospecific aggregation kinetics of colloids we took into account discreteness of receptors on single particles. The population dynamics was modeled using Monte Carlo simulation based on Gillespie stochastic algorithm modified for aggregation kinetics. When a small number of receptors are occupied on a single particle the kinetics simulation resulted in significant deviation from that of the continuous model.

ACKNOWLEDGMENTS

The work on analytical approximation of the diffusion limited rate constant of the aggregation of particles with several active sites was supported by Russian Foundation for Basic Research (Grant No. 12-04-00737-a), whereas Russian Science Foundation (Grant No. 14-15-00155) supported theoretical simulations of immunoagglutination kinetics. The development of the Monte Carlo stochastic simulation algorithm of Gillespie for aggregation was supported by the Program of the President of the Russian Federation for State Support of the Leading Scientific Schools (Grant No. NSh-2996.2012.4) and by the Stipend of the President of Russian Federation for young scientists.

- ¹Q. Chen, S. C. Bae, and S. Granick, *Nature (London)* **469**, 381 (2011); A. Blaaderen, *ibid.* **439**, 545 (2006); A. W. Wilber, J. P. K. Doye, A. A. Louis, and A. C. F. Lewis, *J. Chem. Phys.* **131**, 175102 (2009); **131**, 175101 (2009); J. M. Tavares, L. Rovigatti, and F. Sciortino, *ibid.* **137**, 044901 (2012); A. Giacometti, F. Lado, J. Largo, G. Pastore, and F. Sciortino, *ibid.* **132**, 174110 (2010).
- ²M. V. Smoluchowski, *Z. Phys. Chem.* **92**, 129 (1917); R. M. Ziff, E. D. McGrady, and P. Meakin, *J. Chem. Phys.* **82**(11), 5269 (1985).
- ³M. S. Bowen, M. L. Broide, and R. J. Cohen, *J. Colloid Interface Sci.* **105**(2), 605 (1985).
- ⁴J. H. Zanten and M. Elimelech, *J. Colloid Interface Sci.* **154**(1), 1 (1992); J. W. Virden and J. C. Berg, *ibid.* **149**(2), 528 (1992); I. V. Surovtsev, M. A. Yurkin, A. N. Shvalov, V. M. Nekrasov, G. F. Sivolobova, A. A. Grazhdantseva, V. P. Maltsev, and A. V. Chernyshev, *Colloids Surf., B* **32**, 245 (2003).
- ⁵E. Pefferkorn and R. Varoqui, *J. Chem. Phys.* **91**(9), 5679 (1989); D. A. Weitz and M. Oliveria, *Phys. Rev. Lett.* **52**, 1433 (1984); M. Kolb, R. Botet, and R. Jullien, *ibid.* **51**, 1123 (1983); T. A. Witten and L. M. Sander, *Phys. Rev. B* **27**, 5686 (1983); P. Meakin, *Adv. Colloid Interface Sci.* **28**(4), 249 (1987).
- ⁶R. C. Ball, D. A. Weitz, T. A. Witten, and F. Leyvraz, *Phys. Rev. Lett.* **58**(3), 274 (1987); G. K. Schulthess, G. B. Benedek, and R. W. DeBlois, *Macromolecules* **13**, 939 (1980); D. Johnston and G. B. Benedek, in *Kinetics of Aggregation and Gelation*, edited by F. Family and D. P. Landau (Elsevier, Amsterdam, 1984), p. 181; D. W. Schaefer, J. E. Martin, P. Wiltzius, and D. S. Cannell, *Phys. Rev. Lett.* **52**, 2371 (1984).
- ⁷V. M. Berdnikov and A. B. Doktorov, *Chem. Phys.* **69**, 205 (1982).
- ⁸J. A. Molina-Bolivar and F. Galisteo-Gonzalez, *J. Macromol. Sci., Polym. Rev.* **45**, 59 (2005).
- ⁹C. J. van Oss, *J. Immunoassay* **21**(2–3), 143 (2000).
- ¹⁰R. Zwanzig and A. Szabo, *Biophys. J.* **60**(3), 671 (1991).
- ¹¹W. Scheider, *J. Phys. Chem.* **76**(3), 349 (1972); M. Tachiya, *Radiat. Phys. Chem.* **21**, 167 (1983); A. I. Shushin, *J. Chem. Phys.* **110**, 12044 (1999); S. Saddawi and W. Strieder, *ibid.* **136**, 044518 (2012); J. Uhm, J. Lee, C. Eun, and S. Lee, *ibid.* **125**(5), 054911 (2006); C. Y. Son, J. Kim, J.-H. Kim, J. S. Kim, and S. Lee, *ibid.* **138**(16), 164123 (2013); S. D. Traytak, *Chem. Phys. Lett.* **453**, 212 (2008).
- ¹²A. V. Barzykin and A. I. Shushin, *Biophys. J.* **80**, 2062 (2001).
- ¹³A. B. Doktorov and N. N. Lukzen, *Chem. Phys. Lett.* **79**, 498 (1981).
- ¹⁴S. I. Temkin and B. I. Yakobson, *J. Phys. Chem.* **88**(13), 2679 (1984).
- ¹⁵K. L. Ivanov and N. N. Lukzen, *J. Chem. Phys.* **128**, 155105 (2008).
- ¹⁶H. C. Berg and E. M. Purcell, *Biophys. J.* **20**(2), 193 (1977).
- ¹⁷A. I. Burshtein, A. B. Doktorov, and V. A. Morozov, *Chem. Phys.* **104**, 1 (1986).
- ¹⁸K. Solc and W. H. Stockmayer, *J. Chem. Phys.* **54**, 2981 (1971).
- ¹⁹K. Solc and W. H. Stockmayer, *Int. J. Chem. Kinet.* **5**, 733 (1973).
- ²⁰J. M. Schurr and K. S. Schmitz, *J. Phys. Chem.* **80**, 1934 (1976); R. Samson and J. M. Deutch, *J. Chem. Phys.* **68**, 285 (1978); A. I. Burshtein and B. I. Yakobson, *Int. J. Chem. Kinet.* **12**, 261 (1980); D. Shoup, G. Lipari, and A. Szabo, *Biophys. J.* **36**(3), 697 (1981); A. B. Doktorov and B. I. Yakobson, *Chem. Phys.* **60**(2), 223 (1981).
- ²¹G. Wilemski and M. Fixman, *J. Chem. Phys.* **58**, 4009 (1973); M. Doi, *Chem. Phys.* **11**, 115 (1975).
- ²²O. G. Berg, *Biophys. J.* **47**(1), 1 (1985).
- ²³S. H. Northrup, *J. Phys. Chem.* **92**(20), 5847 (1988).
- ²⁴R. M. Ziff, in *Kinetics of Aggregation and Gelation* (Elsevier, Amsterdam, 1984), p. 191.
- ²⁵M. L. Broide and R. J. Cohen, *J. Colloid Interface Sci.* **153**(2), 493 (1992).
- ²⁶H. Holthoff, A. Schmitt, A. Fernandez-Barbero, M. Borkovec, M. A. Cabrerizo-Vilchez, P. Schurtenberger, and R. Hidalgo-Alvarez, *J. Colloid Interface Sci.* **192**(2), 463 (1997).
- ²⁷D. E. Guinapp and J. S. Schultz, *J. Phys. Chem.* **90**(14), 3282 (1986).
- ²⁸D. T. Gillespie, *J. Atmos. Sci.* **32**, 1977 (1975).
- ²⁹D. T. Gillespie, *J. Comput. Phys.* **22**, 403 (1976).
- ³⁰I. J. Laurenzi and S. L. Diamond, *Biophys. J.* **77**(3), 1733 (1999).
- ³¹M. A. Gibson and J. Bruck, *J. Phys. Chem.* **104**, 1876 (2000).